https://doi.org/10.5194/egusphere-2024-316
Preprint. Discussion started: 13 February 2024

Attribution of aerosol particle number size distributions to major sources using a 11-year-long urban dataset

Máté Vörösmarty[1], Philip K. Hopke[2,3], and Imre Salma[4]

[1] Hevesy György Ph.D. School of Chemistry, Eötvös Loránd University, Budapest, Hungary
[2] Department of Public Health Sciences, University of Rochester School of Medicine and Dentistry, Rochester, NY, USA
[3] Institute for a Sustainable Environment, Clarkson University, Potsdam, NY, USA
[4] Institute of Chemistry, Eötvös Loránd University, Budapest, Hungary

Correspondence: Imre Salma (salma.imre@ttk.elte.hu) and Máté Vörösmarty (vmate6@student.elte.hu)

Abstract. Source apportionment was performed using size segregated particle number concentrations (PNCs) in 27 size channels over the diameter range of 6–1000 nm augmented by air pollutants all with a time resolution of 1 h in the urban background of Budapest for 11 full years in separate seasons. The input dataset was corrected for the effect of the local meteorology by dispersion normalization using the ventilation coefficient defined as the planetary boundary mixing layer height multiplied by the wind speed. Both the uncorrected and dispersion-corrected datasets were evaluated using positive matrix factorization. Six source types including nucleation, two road vehicle emission sources separated into a semi-volatile fraction and a solid core fraction, diffuse urban source, secondary inorganic aerosol (SIA), and ozone-associated particles were identified, characterised, and quantified. The ventilation correction substantially modified the input concentrations, while the differences in the corrected-to-uncorrected ratios for the contributions remained within 5 %. The overall mean relative contribution of the road traffic emission sources was 60 %, and did not show considerable seasonal variability. Nucleation was responsible for 20 % of the PNC annually as a lower estimate. It exhibited a compound character consisting of photochemically induced nucleation and traffic-related nucleation. The former process occurs on regional or urban spatial scales around noon, whereas the latter process happens when the gas-phase vapours in the vehicle exhaust cool, and the resulted supersaturated vapours nucleate outside the source. Its relative contributions were maximal in spring (somewhat smaller in summer and autumn) and minimal in winter. The contributions from the SIA and the urban diffuse source types were approximately 10 % in spring, summer, and 12–15 % in autumn and winter, respectively. The O_3-associated secondary aerosol made up the smallest (6 %) portion of particles on an annual basis. Directionality variations investigated by conditional bivariate probability function analysis were used to locate the likely source areas, and showed considerable spatial variations in the source origin.

https://doi.org/10.5194/egusphere-2024-316
Preprint. Discussion started: 13 February 2024

1 Introduction and objectives

Particulate matter (PM) plays a vital role in the urban air quality worldwide. It is often quantified by the mass of particles, which is established as a key or criteria air pollutant (EU EEA, 2023; US EPA, 2023). Coarse- and accumulation-mode particles make up most PM mass, whereas the mass contribution of the ultrafine (UF) particles (with $d < 100$ nm) is negligible (e.g., Salma et al., 2002). Despite that UF particles make up > 80 % of total particle numbers in cities (Trechera et al., 2023). At relatively low PM mass and high UF particle concentrations, it is the particle number that represents the potential danger to human health better than the PM mass. Although there is less information on the role of UF particles in health effects, there are toxicological (Oberdörster et al., 2005; HEI Review Panel, 2013), clinical (Chalupa et al., 2004) and epidemiologic (Kreyling et al., 2006; Wang et al., 2019a) studies, which suggest that these particles can cause adverse health effects. Inhalation of very small insoluble particles can particularly lead to excess health risk relative to coarse or fine particles of the similar chemical composition (Oberdörster et al., 2005; HEI Review Panel, 2013). This is caused by the vast number of the deposited particles in the respiratory system, their large total surface area and small size (Braakhuis et al., 2014; Salma et al., 2015; Riediker et al., 2019). The World Health Organization identified the UF particles as a potential risk factor for humans (WHO, 2021).

Particle number size distributions (PNSD) can vary considerably over space and time. Formation and atmospheric transformation processes basically contribute to this process. Apart from the vicinity of intensive sources of UF particles, the PNSDs change rates become much slower. Under these balanced conditions, the PNSDs can be separated into such size modes that are associated with source types or aggregate sources (Hopke et al. 2022 and references therein). The PNSDs usually consist of Aitken and accumulation modes. In addition, nucleation mode appears for constrained time intervals. Aitken-mode particles are usually emitted into the air and can contain largely variable portions of semi-volatile components condensed on solid (mostly soot) core (Morawska et al., 2008; Harrison et al., 2019; Rönkkö and Timonen, 2019). Accumulation-mode particles ordinarily result from transformation processes such as condensation growth, physical and chemical ageing or water activation processes of Aitken-mode or nucleated particles. The nucleation mode can be associated with new aerosol particle formation (NPF) and growth events (Kulmala et al., 2003).

Primary pollutants (including particle number concentrations and size distributions) can also be affected by meteorological processes such as atmospheric mixing and transport due to their dispersion (dilution or enrichment). The dispersion is often governed by solar radiation through planetary boundary mixing layer

https://doi.org/10.5194/egusphere-2024-316
Preprint. Discussion started: 13 February 2024

height (MLH), wind or precipitation (Andronanche, 2004; Kumar et al., 2011). These conditions can substantially affect both larger, geographically closed areas such as orographic basins and smaller territories such as cities or valleys (Leahey, 1972; Salma et al., 2020). The dispersion of primary particles is essentially related to the available air volume in which they are mixed (Holzworth, 1967; Ashrati et al., 2009). In cities, this volume is determined by the MLH and WS in the first order approximation. It is noted that meteorological variables may affect secondary pollutants and particles in a more complex and separate way with respect to the primary pollutants and particles.

The spatial and temporal diversity and dynamics of the formation and transformation processes, and of meteorological conditions are reflected in the PNSDs as far as both their integrated concentration and shape are concerned (Li et al., 2023). Thus, size distributions can be used for identifying and quantifying various source types. These basically differ from the sources dominating the PM mass. The particle number concentrations are nonconservative compared to the PM mass. Attribution of PNSDs to different source types and their quantification are desirable and essential since many basic properties, atmospheric behaviour of particles as well as their health, environmental and climate effects depend on their number (and not their mass) concentration (e.g., Ibald-Mulli et al., 2002; Meng et al., 2013; Corsini et al., 2019). Source apportionment can also yield valuable knowledge for creating air quality regulatory strategies for particle numbers or their source specific exposure metrics. Therefore, there is recently a considerable and increasing scientific interest in source apportionment studies on PNSDs (Beddows et al., 2019; Dai et al., 2021; Hopke et al., 2022; Teinilä et al., 2022; Conte et al., 2023; Crova et al., 2024; Rowell et al., 2024). However, studies based on multiple-year-long data are still scarce (de Jesus et al, 2020).

Source apportionments can be achieved by multivariate modelling (Hopke, 1991). Positive matrix factorisation (PMF; Paatero and Tapper, 1993, 1994) is one of the most widely used, well established and efficient technique for this (Hopke, 2016; Hopke et al., 2020). The PMF modelling was successfully applied to mass concentrations of aerosol constituents and gases (e.g., Viana et al., 2008; US EPA, 2014; Hopke et al., 2020). The main differences between the PMF deployed on particle number size distribution data with respect to that on mass concentrations include different approaches in handling zero data and values below the detection limit, and in estimating the observation uncertainties (Ogulei et al., 2007).

To study the phenomenon of the urban atmospheric NPF and growth in Budapest, PNSDs in the diameter range of 6–1000 nm, meteorological properties and air pollutants were measured for 11 full measurement years. They belong to the longest critically evaluated urban datasets of this kind in the world. Utilising

https://doi.org/10.5194/egusphere-2024-316
Preprint. Discussion started: 13 February 2024

this readily available dataset for source apportionment by PMF method offers different and comprehensive insights into the sources of particle numbers. Such long-term observations are particularly valuable as they can statistically reveal information which were hidden in the noise on shorter time scales (Kulmala et al., 2023). The main objectives of this study are 1) to present and discuss the results and experience gained from the source apportionment of PNSDs by applying the PMF method for separate seasons in Budapest; 2) to quantify the effect and importance of the dispersion correction; 3) to interpret the main sources and their spatial distributions; and 4) to determine the relative contributions from the sources. Our conclusions can also contribute to the general understanding of the source, transformation and transport processes of particle numbers in cities and to developing novel air quality regulatory policy for them.

2 Methods

2.1 Experimental part and data treatment

The measurements were performed at two urban sites in Budapest. Most of them were conducted at the Budapest platform for Aerosol Research and Training (BpART) Laboratory (47°28'29.9" N, 19°3'44.6" E; 115 m above mean sea level, m.s.l.) of the Eötvös Loránd University (Salma et al., 2016a). The measurement site is located 85 m from the River Danube, which flows through the city centre. The location represents a typical urban background site due to its geographical and meteorological conditions. The other measurement site was in a wooden area of the Konkoly Astronomical Observatory (47°30'00" N, 18°57'47" E; 478 m above m.s.l.) at the NW border of the city. Since the prevailing wind direction in the area is NW, the latter site represents the near-city background.

The PNSDs were measured using a flow-switching-type differential mobility particle sizer (DMPS) system, which operates in the electrical mobility diameter range from 6 to 1000 nm in the dry state of particles (relative humidity, RH < 30 %) separating the particles into 27 size channels with a time resolution of τ = 8 min (Salma et al., 2011, 2016b, 2021). The nominal diameters of the 27 channels are 6.0, 7.3, 8.9, 10.8, 13.2, 16.0, 19.5, 23.7, 28.9, 35.2, 42.9, 52.1, 63.4, 77.2, 93.9, 114, 139, 169, 206, 250, 304, 371, 451, 550, 670, 816, and 994 nm. This list facilitates the exact interpretation of the factor profiles in Figs. 2a–4a and S5a–S7a. The concentrations of NO, NO_x/NO_2, CO, O_3, SO_2, PM_{10} mass were acquired from the closest measurement stations of the National Air Quality Network located 4.5 km from the urban background site and 6.9 km from the near-city background site in the upwind prevailing direction (Salma et al., 2020). The time resolution of these measurements was 1 h. Air temperature (*T*), RH, wind speed (WS), wind direction (WD) and global radiation were measured at the BpART Laboratory and above the

https://doi.org/10.5194/egusphere-2024-316
Preprint. Discussion started: 13 February 2024

rooftop level of the building complex (at a height of 45 m above the nearest street). The wind data above the rooftop level were utilised in the present study and were recorded by standardized sensors (WAA15A and WAV15A, both Vaisala, Finland) with τ = 10 min. Mixing layer height data (τ = 1 h) were extracted from the Copernicus Climate Change Service (ERA5 Family datasets, ECMWF reanalysis; Hersbach et al., 2023).

The data were expressed in local time (UTC+1 or daylight-saving time UTC+2). This was chosen since the activities of the inhabitants greatly influence the atmospheric concentrations and size distributions in cities (Mikkonen et al., 2020). Hourly mean particle number size distributions were derived from the experimental data to reduce their fluctuations and the number of the missing data. Atmospheric concentrations in each size channel and of the total particle number concentrations ($N_{6–1000}$) were calculated and further evaluated. The investigated time interval involved 11 full measurement years (Table S1). The data from the two urban sites were evaluated together. The residuals and the goodness of the fits in the PMF modelling did not indicate significant differences between the respective factor profiles in the urban background and near-city background. Additionally, this multi-site approach is expected to improve the efficiency of the source apportionment (Pandolfi et al., 2010; Dai et al., 2020; Harni et al., 2023). The median $N_{6–1000}$ and atmospheric concentrations of pollutants over the measurement years are also summarised in Table S1. The overall dataset was finally split into separate subsets for meteorological seasons (March, April, May as spring, June, July, August as summer, September, October, November as autumn and December, January, February as winter) to fulfil one of the basic requirements of the PMF method on the consistency of the source profile over the time interval considered (Zhou et al., 2004; Ogulei et al., 2007). The missing concentration values in the input dataset were replaced by the medians with 3-times the measurement uncertainty of the seasonal dataset. The data coverage for the input data was typically > 85 %. The total number of observations for the PNSDs are shown in Fig. S2. The seasonal means and standard deviations (SDs) of the meteorological properties are summarised in Table S2.

2.2 Source apportionment modelling

The source apportionment was performed using the PMF method with the equation solver Multilinear Engine 2 (ME-2) as described by Hopke et al. (2023). The method decomposes the input dataset into a factor (source) profile matrix and a factor contribution matrix with a user-specified factor number based on the covariances between the variables. The PMF iteratively optimizes the objective parameter Q, which is calculated on the individual residuals (e) and the uncertainties (s) for the observation i and variable j:

$$Q = \sum_{i=1}^{m} \sum_{j=1}^{n} \left(\frac{e_{ij}}{s_{ij}}\right)^2, \quad (1)$$

https://doi.org/10.5194/egusphere-2024-316
Preprint. Discussion started: 13 February 2024

where m and n are the maximum number of observations and variables, respectively. Q_{true} was calculated with all data points, whereas Q_{robust} was determined excluding the poorly fitted data points (i.e. when their uncertainty-scaled residuals were greater than 4). The uncertainties of the particle number concentrations in a size channel j were estimating as (Ogulei et al., 2007):

$$\sigma_{ij} = (A * \alpha) * \left(N_{ij} + \bar{N}_j\right), \quad (2)$$

$$s_{ij} = \sigma_{ij} + C_3 * N_{ij}, \quad (3)$$

where σ is the estimated individual measurement uncertainty for an observation, N represents the observed concentration, $\bar{N}$ is the arithmetic mean of the observed concentrations in the respective variable, α is constant (of 0.01), which value is fine-tuned by A for particle number concentrations, s is the overall uncertainty matrix, and C_3 is constant (0.01 for size channels, 0.2 for $N_{6–1000}$ and 0.15 for air pollutants), which is also tuned around these nominal values. These selections and relationships are widely accepted in the PNSD source apportionment studies. The addition of the pollutants is beneficial for the PMF as the new quantities provide insights into the sources or atmospheric processes that produce the measured size distributions, and reduce the rotational ambiguity of the model by complementing the edge points (Paatero, 1999; Hopke, 2016). Specifying too low uncertainties relative to the true error level results in overweighting those datapoints, while larger uncertainties yields downweighting (Hopke, 2020). Moderate downweighting exerts less sensitive effect on the modelling results than overweighting, and the overdetermined uncertainties can also obscure the concentration data.

Dispersion of the atmospheric concentrations due to the changes of meteorological conditions can result in additional covariance as well. This effect can be corrected for by dispersion normalization of the input dataset with the ventilation coefficient (VC; Ashrati et al., 2009). In this approach, the available air volume for the atmospheric dispersion is proportional to the product of the MLH_i and the vectorial mean of the wind speed (u_i) for the observation i:

$$\mathrm{VC}_i = \mathrm{MLH}_i * u_i. \quad (4)$$

The concentration data (C_i) were multiplied by the ratio of the corresponding VC_i and its seasonal mean value $\overline{\mathrm{VC}}$ (called ventilation coefficient ratio):

$$C_{Vi} = C_i * \frac{\mathrm{VC}_i}{\overline{\mathrm{VC}}}. \quad (5)$$

After completing the PMF analysis on the corrected dataset, the derived source contributions were divided by the respective VC ratios to obtain the real contributions. The source apportionment modelling was performed independently both on the uncorrected and corrected concentrations. The results derived from

https://doi.org/10.5194/egusphere-2024-316
Preprint. Discussion started: 13 February 2024

the uncorrected dataset (i.e. C_i concentrations) are referred as uncorrected (or traditional) PMF data, while those obtained from the corrected dataset (C_{Vi} concentrations) are denoted as dispersion-corrected (DC-) PMF data.

The PMF solutions were explored in 50 runs with different configurations for each dataset. The factor count was changed between four to twelve; the uncertainty parameters were modified from 0.01 to 0.05 for ($\alpha \times A$), and between 0.01 and 0.1 for C_3. Increased uncertainty settings were adopted for the smallest (< 10 nm) and the largest (> 800 nm) size channels since their uncertainties were proven to be larger (Wiedensohler et al., 2012), and for the pollutants since they were set as weak variables. The final solution was reached through a trial-and-error approach. Additional error estimations were run using bootstrap and displacement analyses. From the analysis point of view, the best solution (approved later as the final solution) was chosen to meet the criteria that the convergence is achieved in the robust manner; its Q_{true} and Q_{robust} diagnostic values are among the lowest values; the scaled residuals are distributed preferably normally between –3 and +3; and that the goodness of the fit (expressed by the coefficient of determination, R^2) for the strong variables are reasonable (typically > 0.85). From the interpretation aspect, the main requirements were that the solution is physically interpretable based on the size profiles; is acceptable as far as directional probability function plots are concerned, and shows sensible diel patterns, weekly and annual tendencies.

Spatial variations of the source intensities and other properties were derived by conditional bivariate probability function (*polarPlot()*) of the 'openair' package (Carlsaw and Ropkins, 2012; Uria-Tellaexte and Carlsaw, 2014). The method utilizes WS and WD data to create plots of directionality. The plots derived from the uncorrected and corrected PMF modelling were compared using the *polarDiff()* function of the package. Further statistical evaluations and presentations were accomplished by a laboratory-developed application AeroSoLutions2 in conjunction with the Accord.NET Framework (Souza, 2014).

3 Results and discussion

3.1 Dispersion correction and its effect on the input dataset

The mean diel variations of the ventilation coefficient ratio and of its MLH and WS constituents are shown in Fig. S1 separately for seasons. They all exhibited a pattern consisting of a broad band during the daylight period. The MLH curves showed the maximum value in summer, a lower, but close time series in spring, the minimum value in winter and a close, but somewhat higher curve in autumn (Fig. S1a). During the evening and night, the curves were similar to each other. The WS time series displayed

https://doi.org/10.5194/egusphere-2024-316
Preprint. Discussion started: 13 February 2024

maxima in spring, smaller and fairly similar levels in summer and winter, and minima in autumn (Fig. S1b). As a result, the time series of the VC_{ratio} over the peak region were similar to each other in summer, spring and autumn, while the ratios in winter were smaller than for the other seasons (Fig. S1c). The order of the levels of the VC time series during the evening and night were just the opposite to those over the daylight. The VC_{ratio} data were above unity (up to 2.5 in summer) approximately from 07:00 to 15:00 UTC+1 in all seasons, whereas they were < 1 (down to 0.25 in summer) outside this time interval. These all indicate that the dispersion correction can be substantial in summer, spring and autumn, and it is smaller, but still relevant in winter.

The effect of the dispersion correction on the PMF input data are demonstrated by the diel variations of the uncorrected and dispersion-corrected $N_{6–1000}$ for separate seasons (Fig. 1). The structure of the uncorrected curves (Fig. 1a) was discussed and explained earlier (Salma et al., 2011, 2020; Thén and Salma, 2021). In summary, they show three peaks; early-morning peak and evening peaks at the rush hours of 06:00–08:00 and 18:00–21:00, respectively, largely generated by vehicular road traffic, and a midday peak primarily produced by NPF events driven by photochemistry. The concentrations from 23:00 to 05:00 monotonically decreased and were virtually identical to each other. The curve in summer seems to be below the other lines during the daylight period.

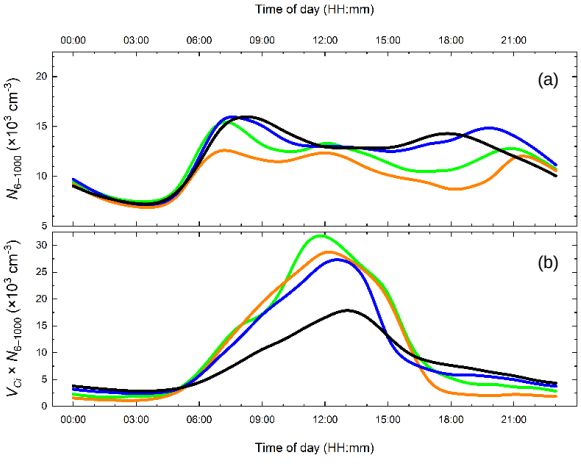

Figure 1. The mean diel variation of the uncorrected ($N_{6–1000}$; a) and dispersion-corrected total particle number concentrations ($VC_i \times N_{6–1000}$; b) separately for spring, summer, autumn and winter.

The concentrations and shape of the dispersion-corrected diel curves were vastly different from the uncorrected lines (Fig. 1b). They all consisted of a broad, single structured peak. The largest maximum

https://doi.org/10.5194/egusphere-2024-316
Preprint. Discussion started: 13 February 2024

of the peaks was observed in spring, the curves in summer and autumn were somewhat lower and similar to each other, while the peak in winter was substantially lower than in the other seasons. The shift in the timing of the maxima was influenced by the clock change for the daylight-saving periods. The curves exhibited monotonically decreasing tendency in evening and reached a constant level during the night. The concentrations of the corrected data during evening and night were smaller, while their levels during the daylight period were larger than the uncorrected levels (as is expected from the VC_{ratio} time series; Fig. S1c). These results emphasize that the input data for the PMF modelling became different after the dispersion-correction from the uncorrected dataset and better reflected the actual emission patterns.

3.2 Interpretation of the factors

The regression lines for the measured and uncorrected modelled $N_{6–1000}$ are show in Fig. S2. The curves and their statistics indicate that the PMF modelling yielded reasonable agreement with the data. Based on the selection criteria described in Sect. 2.2, six-factor solutions were accepted for both the uncorrected and dispersion-corrected datasets and for each season. More factors resulted in unreasonable splitting of some factors (even in winter), whereas a smaller number of factors yielded questionable merging the factors. The approved final solutions represent physically meaningful and sensible approximation for Budapest. The PMF results derived from the uncorrected input data are interpreted in Sects. 3.2.1–3.2.5. The time tendencies and conditional bivariate probability plots of the outcomes obtained from the DC-PMF modelling indicated qualitatively comparable properties and behaviours to them.

3.2.1 Nucleation

The factor associated with the smallest particles in our experimental setup was characterised by a single mode in the source profile with a diameter range from 6 to 25 nm (Fig. 2a). This range ordinarily represents the nucleation mode in NPF studies (Kerminen et al., 2018) and corresponds to its typical time-averaged evolution (e.g., Salma and Németh, 2019). The factor contributions (concentrations) were the largest in spring and the smallest in winter (Fig. 2b). This variation coincides with the relative occurrence frequency of the NPF events in the larger Budapest area (the Carpathian Basin; Salma et al., 2016b, 2021). The diel variations of the $N_{6–1000}$ from this factor showed the highest intensity at 12:00 in all seasons with the largest peak in spring and with the smallest peak (if any) in winter (Fig. 2c).

Nevertheless, the time series unambiguously indicated additional peaks in the early-morning and evening rush hours in addition to the midday peak (Figs. 2c and S3a, b). The factor also exhibited non-negligible association with NO, NO_2 and CO with varying degrees (Fig. 2a). These results suggest that there is connection between this factor and the vehicular road traffic, particularly in non-winter seasons. The

https://doi.org/10.5194/egusphere-2024-316
Preprint. Discussion started: 13 February 2024

compound character of the factor was recognised earlier (Rivas et al., 2020). In our results, the importance of the traffic-related sub-factor was higher on weekdays compared to weekends (particularly in the early-morning rush hours on Sunday) when the traffic intensity is lower (Fig. S3a). The small peak at ca. 110 nm could be generated by heterogeneous nucleation of semi-volatile organic compounds on primary soot particles, which is a likely process in rapidly diluting and cooling air due to the turbulence caused by road vehicles. It could equally be a modelling artefact since in this diameter range, enlarged displacement intervals were noticed.

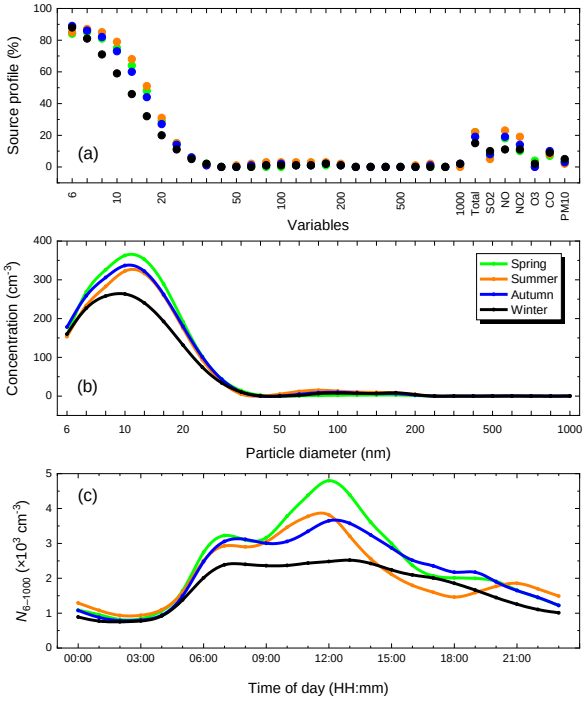

Figure 2. Relative factor profile (a), factor contribution to the particle number concentrations in the size channels (b), and the mean diel variation of the total particle number concentrations ($N_{6–1000}$; c) assigned to the compound nucleation source in spring, summer, autumn and winter. The exact diameters of the size channels are listed in Sect. 2.1.

This factor is interpreted as nucleation that is a combination of photochemically induced nucleation with traffic-related nucleation. The former process occurs on a regional or urban spatial scale around noon. In our results, this was also associated with strong southern winds (Fig. S9) consistently with our earlier conclusions (Németh and Salma, 2014). Higher WS values often represent cleaner air in the city centre, and the relationship between high WS and NPF occurrence is in line with our earlier observations in Budapest (Salma et al., 2021). The traffic-related nucleation in cities can happen when the gas-phase vapours and gases in the exhaust of road vehicles cool, and the resulted supersaturated vapours can

https://doi.org/10.5194/egusphere-2024-316
Preprint. Discussion started: 13 February 2024

nucleate outside the source (Charron and Harrison, 2003). The process yields nucleated particles which have been called delayed primary particles (Rönkkö et al., 2017). This explains why the traffic circulation patterns showed up in the time series of this factor.

3.2.2 Traffic emissions

There were two factors showing unimodal source profile each in the Aitken mode, which indicates that these were primary particles (Figs. 3a and 4a). Both factors exhibited considerable contributions to NO, NO_2 and CO as well. These gases are related to combustion processes. The time series of the concentration contributions of the two factors clearly followed the daily and monthly patterns of the vehicle circulation in Budapest, and were larger on weekdays than on weekends (Figs. 3c, 4c, S4 and S5). They both can be related to direct emissions from motor vehicles. There were, however, several major differences between the two factors, which discriminate them from each other.

One of the road traffic emission factors showed the largest contributions to the particles with a diameter of 25–35 nm (Fig. 3a). Its concentration contributions resulted in a mode, which was the smallest in summer (Fig. 3b). The diel variability of the factor also showed different magnitudes over seasons. The seasons were characterised by diverse seasonal mean T values from 3 to 23 °C (Table S2). The contributions to the total particles were the largest in winter, large in autumn and spring, and the smallest in summer (Fig. 3c). This points to the presence of chemical constituents with semi-volatile physicochemical properties. The curves for summer contained a midday peak in addition to the rush-hour peaks, which could be related to the altered traffic pattern (with a peak at noon) in Budapest on summer holidays. The source origin was shifted to more regional scales with WS in spring, and showed local origin in winter (Fig. S9).

Based on these reasons and consistently with earlier conclusions (Robinson et al., 2007; Morawska et al., 2008; Rönkkö et al., 2017; Harrison et al., 2018; Rowell et al., 2024), this factor is interpreted as emission source of semi-volatile aerosol fraction from road vehicle traffic (traffic-svf). Considering that diesel vehicles are responsible for much of the exhausted particle numbers from road traffic in Europe (Damayanti et al., 2023), the important concrete source is the semi-volatile emissions from diesel engines. Emissions from gasoline combustion in spark-ignited engines likely contribute as well, which can be inferred from the differences in the diel patterns of the two traffic-related emission sources over the week (Figs. S4a vs. S5a). The naming and detailed interpretation of this factor varies in the literature such as emissions from gasoline vehicles (Liu et al., 2014) or fresh traffic emissions (Rivas et al., 2020) or Traffic 1 (Hopke et al., 2022).

https://doi.org/10.5194/egusphere-2024-316
Preprint. Discussion started: 13 February 2024

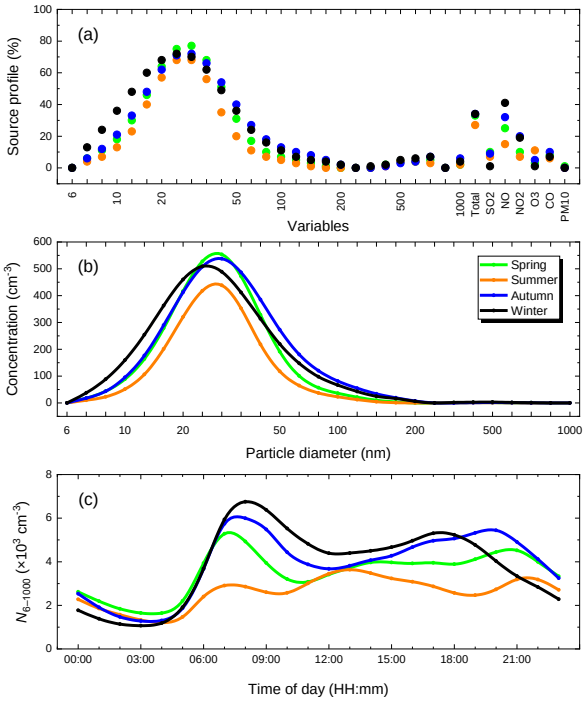

Figure 3. Relative factor profile (a), factor contribution to the particle number concentrations in the size channels (b), and the mean diel variation of the total particle number ($N_{6–1000}$; c) assigned to the source of semi-volatile aerosol species emitted by vehicle road traffic (traffic-svf) for spring, summer, autumn and winter. The exact diameters of the size channels are listed in Sect. 2.1.

The other road traffic emission factor yielded a source profile in a broader diameter interval, actually with a plateau over 65–140 nm, than the traffic-svf source (Fig. 4a). The factor also yielded higher contributions to SO_2 and PM_{10} mass. Its contributions to particle size channels exhibited a single mode with a diameter of 90 nm, which were more stable over the seasons as far as the magnitude and shape are concerned (Fig. 4b). The shares of this factor on the $N_{6–1000}$ did not seem to be influenced by the air temperature in the seasons (Fig. 4c). The diel curves were shifted in the horizontal direction due to the clock adjustments because of the daylight-saving periods. The source origin was related to smaller WS; hence, it remained on more local spatial scale in spring and winter (Fig. S9).

https://doi.org/10.5194/egusphere-2024-316
Preprint. Discussion started: 13 February 2024

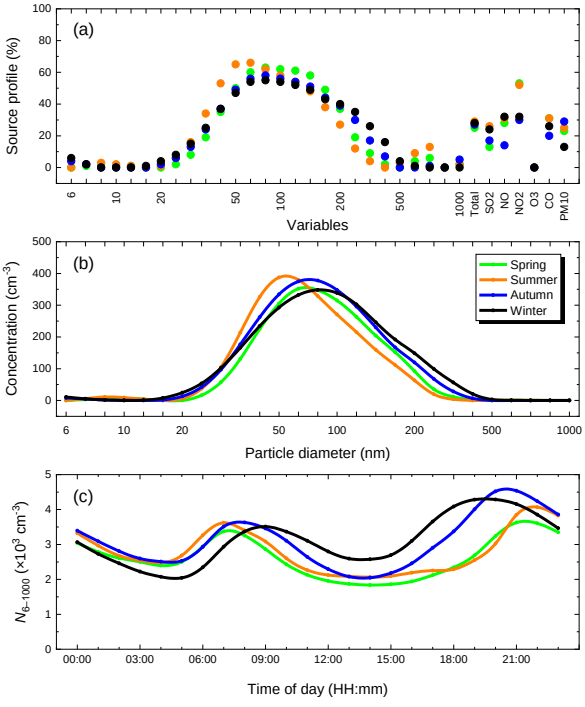

Figure 4. Relative factor profile (a), factor contribution to the particle number concentrations in the size channels (b), and the mean diel variation of the total particle number ($N_{6–1000}$; c) assigned to the source of solid aerosol species emitted by vehicle road traffic (traffic-sf) for spring, summer, autumn and winter. The exact diameters of the size channels are listed in Sect. 2.1.

Based on these reasons and consistently with the earlier studies (Maricq et al., 2002; Rönkkö et al., 2017; Damayanti et al., 2023; Rowell et al., 2024), this factor is interpreted as the source of solid aerosol species emitted by vehicle road traffic (traffic-sf). These particles likely consist of a soot core coated with varying amounts of low-volatility organics or inorganic compounds. The most important source contributing to this factor are the emissions from heavy- and light-duty vehicles (Zhang et al., 2020), which typically contain diesel-powered engine. Chemically and physically aged traffic particles can be partly involved as well (Robinson et al., 2007). The naming and the detailed interpretation of this factor varies in the literature, e.g., emissions from diesel vehicles (Ogulei et al., 2007) or Traffic 2 (Hopke et al., 2022).

3.2.3 Diffuse urban source

Another factor showed a profile with broad peaks at ca. 100 nm and 500 nm (Fig. S6a). It also contained several pollutants including PM_{10} mass (typically in 30 % and up to 50 % in winter) and combustion-related pollutants such as CO, SO_2, NO and NO_2. The profile and contributions also included a low portion of smaller particles (around d = 20 nm). The contributions to concentrations exhibited structured multiple peaks between 70 and 500 nm, which showed elevated levels in winter and autumn, and low values in

https://doi.org/10.5194/egusphere-2024-316
Preprint. Discussion started: 13 February 2024

summer and spring (Fig. S6b). The diel variations from spring to autumn displayed an early-morning peak and an evening peak (with higher level in autumn and lower levels in spring and summer). This pattern could be related to secondary particle formation from gas-phase precursors present in vehicle exhaust when it is fully diluted within the ambient air and oxidised by reactive atmospheric species. In such cases, the particles can grow by condensation. In winter, the diel variation was at the highest level and was featureless (Fig. S6c). The factor was mainly linked to local spatial scales (Fig. S9).

Based on these considerations and earlier studies (Beddows et al., 2015; Beddows and Harrison, 2019; Chandrasekaran et al., 2011; Vratolis et al., 2019; Wang et al., 2019b), this factor is interpreted as source of diffuse (fugitive) urban aerosol. Important concrete sources contributing to it are aged combustion emissions from various boilers and heating equipment used for residential heating or household cooking activities. Burning residual oil and flaming combustion of solid fuels produce distributions with a modal diameter at ca. 100 nm, while efficient combustion of gases and low viscosity oil in stationary burners generate small particles (with a diameter around 20 nm; Hopke et al., 2022 and references therein). This factor was called as urban background (Beddows and Harrison, 2019) or heating (Hopke et al., 2022).

3.2.4 Secondary inorganic aerosol

One of the further factors exhibited a source profile with a relatively narrow mode at the diameter of 800–1000 nm and a broad mode from 50 to 150 nm (Fig. S7a). The larger mode was present in all seasons with similar shapes to each other, but its concentration contributions were all negligible (Fig. S7b). The smaller mode in the source profile was the largest in spring, smaller in summer and missing in autumn and winter (Fig. S7a). Their concentration contributions in the size channels were modest. The shares over a broad size range from 30 to 170 nm were relatively larger with a maximum of 120 cm^{-3} in spring, and with 70 cm^{-3} in summer (Fig. S7b). These contributions were negligible in autumn and winter. An addition mode in the contributions was observed at 250–400 nm, which seemed to be larger in winter than in summer.

Based on these reasons and earlier conclusions (Squizzato et al., 2019; Hopke et al., 2022 and references therein), this factor is ascribed to the sources of secondary inorganic aerosol (SIA), essentially of sulfate and nitrate particles. An important concrete source types in our case could be their secondary formation from gaseous precursors in motor vehicles exhaust (Yoshizumi, 1986). The sulfate particles are produced preferably in summer and spring, when the photochemical activity is larger in a size mode around 100 nm (Yoshizumi, 1986). Consequently, their formation in winter is lower. The ammonium nitrate particles behave contrary to this. They are mainly present in winter, when their thermal dissociation is low and in

https://doi.org/10.5194/egusphere-2024-316
Preprint. Discussion started: 13 February 2024

a size mode at ca. 250 nm (Kadowaki, 1977; Squizzato et al., 2019). The seasonal tendencies and size modes suggest that sulfate particles prevailed to nitrate particles in Budapest. The multimodal directionality plots can indicate the presence of particles of both local and more distant origin. The latter particles were likely influenced by gas-to-particle conversion or other atmospheric or cloud processing (Ogulei et al., 2007; Kasumba et al., 2009; Squizzato et al., 2019).

3.2.5 Secondary aerosol associated with high-ozone conditions

There was a factor associated with remarkably high O_3 (> 80 %) and high SO_2 (40–60 %) contents. It also showed a major mode in the size channels at the diameters of ca. 200 nm in summer (Fig. S8a). The corresponding mode in spring was also present, but it became negligible in autumn and winter. This could be caused by the large seasonal variability of O_3 in Budapest (Salma et al., 2020). As far as the factor contributions are concerned, they exhibited a mode at ca. 45 nm in winter and autumn, and a different mode at 150–200 nm in summer and spring (Fig. S8b). However, the absolute concentration contributions to the size channels remained extremely low (< 85 cm^{-3}). These are in line with earlier studies, in which a variety of size patterns with multiple modes were obtained (Ogulei et al., 2007; Liu et al., 2014; Squizzato et al., 2019). The diel variation of the factor intensity during the daylight period in Budapest was similar to the typical daily development of the in situ O_3 concentration in cities (Fig. S8c), and the contributions were higher on weekdays compared to weekends. The directionality plots the factor intensity indicated associations with higher WS (Fig. S9).

This factor cannot be strictly interpreted in a conclusive manner. It is thought to be the appearance of particles from various primary origins that were grown by condensation of secondary vapours generated by photochemical oxidation driven by O_3 (Juozaitis et al., 1996; Hopke et al., 2022). It is indirectly inferred from the diel variations of the contributions to $N_{6–1000}$ in different seasons (Fig. S7c) and from the size modes in the concentration contributions (Fig. S7b) that this source contains substantial fraction of organic compounds. Additional input data on chemical composition would be advantageous to better clarify this factor. This factor was called O_3-rich secondary aerosol in earlier studies (Ogulei et al., 2007; Liu et al., 2014; Squizzato et al., 2019).

3.3 Importance of sources

The seasonal median uncorrected modelled concentrations of total particle number were 7.1, 6.8, 8.2 and 7.8×10^3 cm^{-3} from spring to winter, respectively. The mean source contribution fractions of the total modelled concentrations derived by both the uncorrected and DC-PMF approaches are displayed in Fig.

https://doi.org/10.5194/egusphere-2024-316
Preprint. Discussion started: 13 February 2024

5 for separate seasons. The relative contributions of unaccounted sources with respect to the measured N_{6-1000} were estimated to be ≤ 2 %.

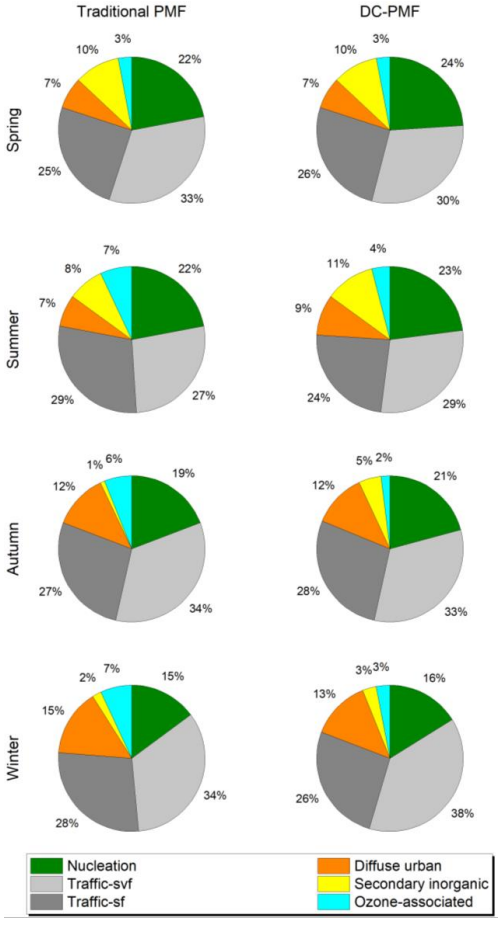

Figure 5. Relative contributions of nucleation, traffic semi-volatile fraction (traffic-svf), traffic solid fraction (traffic-sf), diffuse urban, secondary inorganic aerosol and ozone-associated secondary aerosol sources to the modelled total particle numbers as obtained by the uncorrected (traditional) PMF modelling and the dispersion-corrected (DC-)PMF modelling in spring, summer, autumn and winter.

First we compared the effect of the dispersion correction on the source contributions. The correction substantially enhanced the input concentrations from those sources that are typically active during the daylight periods, and considerably reduced those that originate from the sources mainly active during the nights. At the same time, the differences in the corrected-to-uncorrected ratios for the corresponding contributions remained within 5 % in our datasets for the sources, which shared > 10 % of the N_{6-1000}.

https://doi.org/10.5194/egusphere-2024-316
Preprint. Discussion started: 13 February 2024

Larger differences were only observed for the lower contributions, which raises the question of interpreting the ratios obtained from small absolute values, and may indicate greater uncertainty in these low values.

The overall mean relative contribution of the road traffic emission sources was 59 % (32 % for traffic-svf and 27 % for traffic-sf). They did not show clear trend in seasonal variability. The values and properties are in line with those in other European cities (Beddows et al., 2015; Brines et al., 2015; Dall'Osto et al., 2012; Liu et al., 2014; Posner and Pandis, 2015; Squizzato et al., 2019; Rivas et al., 2020, Hopke et al., 2022 and references therein). Despite that the emissions from vehicles can depend on multiple conditions, for instance on the car fleet, general technical conditions of vehicles, properties of fuels and lubricants used, driving conditions and even on the distance to the nearest road (Rönkkö et al., 2017).

The nucleation source was responsible for 20 % of the particle numbers annually. It was smaller in winter than in the other seasons, particularly compared to the spring and summer. Its share was comparable to our earlier conclusion of 12–27 % (to UF particles) as a lower assessment provided by nucleation strength factor, and to indirect indications (Salma et al., 2017; Thén and Salma, 2022). The present contribution of the nucleation can be, however, considered again as a lower estimate since an extensive portion of the other sources, particularly the SIA in summer and spring and possibly also the urban diffuse source in winter and autumn can be also related to the nucleation. The former source could partly contribute to the nucleation through the vapours generated from gaseous precursors (including SO_2, H_2SO_4 and volatile organics) in the exhausts of road vehicles, ships or airplanes and in the fumes of coal-fired power plants. The urban diffuse source could be linked to nucleated particles via particle growth followed by physical and chemical ageing processes, and possibly coagulation. An unusual type of nucleation events induced by some urban, industrial or leisure activities on sublocal spatial scales with extremely high formation rates was observed in Budapest several times (Salma and Németh, 2019). The contributions from the SIA and urban diffuse source types were approximately 10 % in spring and summer, and 12−15 % in autumn and winter, respectively. They could noticeably further enhance the importance of the nucleation source. The O_3-associated secondary aerosol made up the smallest (6 %) mean contribution on an annual time scale. The shares of the SIA in winter and autumn were 2–3 %. These tendencies are in line with our general understanding of the time behaviour of the related sources and particles.

The directionality plots for the uncorrected PMF results for separate sources are presented in the first two columns of Fig. S9 for the most informative season pairs (for which differences in the $N_{6–1000}$ were the

https://doi.org/10.5194/egusphere-2024-316
Preprint. Discussion started: 13 February 2024

most noticeable). The road traffic emission sources were related to local spatial scales in all seasons except for summer. In this latter case, more distant regions and larger WS values prevailed. The nucleation source in spring (when its occurrence frequency was the largest) was associated with SE direction and high WS. This directionality is coherent with our earlier finding (Németh and Salma, 2014). In winter, its source directionality plot was featureless. The diffuse urban aerosol originated from local spatial scales and low WS in all seasons, which is in accordance with its source interpretation. The SIA was relevant only in spring and summer, with prevailing SE and NW directions, respectively and with high WS values. The intensity of the O_3-associated secondary aerosol source in winter and autumn remained low in the city centre and higher in its outskirt.

The differences in the directionality plots were obtained by subtracting the uncorrected PMF results from the DC-PMF results. They are shown in the third and fourth columns of Fig. S9 for the identical seasonal pair as for the directionality plots. Despite the similar seasonal mean contributions from both the uncorrected and corrected PMF (Fig. 5), there are substantial variations in the plots. The corrected PMF can considerably change the source origins. In this respect, the DC-PMF can provide important added values for interpreting the spatial distribution of the sources. More detailed and reliable interpretations will be feasible after gaining further experience and expertise in the future studies.

4 Conclusions

Six major source types of particle numbers were identified in Budapest. The road vehicle emissions were the largest contributors; they were responsible for approximately 60 % of particles. This source was resolved into a semi-volatile fraction and a solid (soot core) fraction. It seems likely that these two types do not express the emissions from gasoline- and diesel-driven motor vehicles, but they represent two distinct groups of chemical mixtures from both internal combustion engines. Nevertheless, both sources, particularly that containing solid fraction, are dominated by diesel motor vehicles. More importantly, the latter source is characterised by a modal diameter around 90 nm and is expected to contain high portions of insoluble particles. These properties can yield considerably larger lung deposited surface areas than for the traffic-svf or the other sources (except for the urban diffuse source), which results in extraordinary particle burden in the human lung caused by this individual source. Moreover, the surface-active properties of soot core likely represent additional risk for the health outcomes.

The nucleation source was responsible for ca. 20 % of particles as a lower estimate. It displayed a compound character consisting of photochemically induced nucleation and traffic-related nucleation.

https://doi.org/10.5194/egusphere-2024-316
Preprint. Discussion started: 13 February 2024

There is a method available for splitting it into the two specific (sub)sources using NO_x as a proximity marker for vehicle road traffic (Rivas et al., 2020). However, in our datasets the coefficients of correlation between the nucleation intensity and NO_x concentration were typically < 0.2, and adopting this method yielded unusually small photochemically induced nucleation contributions. They are in contrast with our earlier results and other indirect estimations (Thén and Salma, 2022), and with other suggestions as well (Rowell et al., 2024). Therefore, we avoided adopting this estimation for the time of being, and emphasize here the need for developing generally valid splitting methods, and testing them on a variety of datasets.

All particle number size distributions attributed to the sources together with their relevant conjugate size distributions are to be further utilised in an advanced lung deposition model for characterising and quantifying source specific depositions in the human respirators system.

Data availability. The observational data are available from the corresponding author (IS).

Supplement. The supplement related to this article is available online at: *to be completed*.

Author contributions. MV performed the data treatment and modelling, prepared the figures, participated in the interpretation and writing the manuscript. PKH participated in the conceptualization the interpretation of the results and editing. IS provided the dataset, conducted the conceptualization, participated in the interpretation and writing the manuscript. All coauthors contributed to the discussion of the results and provided comments on the manuscript.

Competing interests. The authors declare that they have no conflict of interest.

Financial support. This research has been supported by the Hungarian Research, Development and Innovation Office (grant K132254), and the New National Excellence Program of the Ministry for Culture and Innovation from the source of the National Research, Development and Innovation Fund (ÚNKP-22-3).

References

Andronabusche, C.: Precipitation removal of ultrafine aerosol particles from the atmospheric boundary layer, J. Geophys. Res., 109, D16S07, https://doi.org/10.1029/2003jd004050, 2004.

Ashrafi, Kh., Shafie-Pour, M., and Kamalan, H.: Estimating temporal and seasonal variation of ventilation coefficients, Int. J. Environ. Res., 3, 637–644, 2009.

Beddows, D. C. S., Harrison, R. M., Green, D. C., and Fuller, G. W.: Receptor modelling of both particle composition and size distribution from a background site in London, UK, Atmos. Chem. Phys., 15, 10107–10125, https://doi.org/10.5194/acp-15-10107-2015, 2015.

Beddows, D. C. S. and Harrison, R. M.: Receptor modelling of both particle composition and size distribution from a background site in London, UK – a two-step approach, Atmos. Chem. Phys., 19, 4863–4876, https://doi.org/10.5194/acp-19-4863-2019, 2019.

Braakhuis, H. M., Park, M. V., Gosens, I., De Jong, W. H., and Cassee, F. R.: Physicochemical characteristics of nanomaterials that affect pulmonary inflammation, Part. Fibre Toxicol., 11, 18, https://doi.org/10.1186/1743-8977-11-18, 2014.

Brines, M., Dall'Osto, M., Beddows, D. C. S., Harrison, R. M., Gómez-Moreno, F., Núñez, L., Artíñano, B., Costabile, F., Gobbi, G. P., Salimi, F., Morawska, L., Sioutas, C., and Querol, X.: Traffic and nucleation events as main sources of ultrafine particles in high insolation developed world cities, Atmos. Chem. Phys., 15, 5929–5945. https://doi.org/10.5194/acp-15-5929-2015, 2015.

https://doi.org/10.5194/egusphere-2024-316
Preprint. Discussion started: 13 February 2024

Carslaw, D. C. and Ropkins, K.: openair – An R package for air quality data analysis, Environ. Modell. Softw., 27–28, 52–61, https://doi.org/10.1016/j.envsoft.2011.09.008, 2012.

Chalupa, D. C., Morrow, P. E., Oberdörster, G., Utell, M. J., and Frampton, M. W.: Ultrafine particle deposition in subjects with asthma, Environ. Health Perspect., 112, 879–882, https://doi.org/10.1289/ehp.6851 879–882, 2004.

Chandrasekaran, S. R., Laing, J. R., Holsen, T. M., Raja, S., and Hopke, P. K.: Emission characterization and efficiency measurements of high-efficiency wood boilers, Energy Fuels 25, 5015−5021, https://doi.org/10.1021/ef2012563, 2011.

Charron, A. and Harrison, R. M.: Primary particle formation from vehicle emissions during exhaust dilution in the roadside atmosphere, Atmos. Environ, 37, 4109-4119, https://doi.org/10.1016/S1352-2310(03)00510-7, 2003.

Conte, M., Dinoi, A., Grasso, F. M., Merico, E., Guascito, M. R., and Contini, D.: Concentration and size distribution of atmospheric particles in southern Italy during COVID-19 lockdown period, Atmos. Environ., 295, 119559, https://doi.org/10.1016/j.atmosenv.2022.119559, 2023.

Corsini, E., Marinovich, M., and Vecchi, R.: Ultrafine particles from residential biomass combustion: a review on experimental data and toxicological response, Int. J. Mol. Sci., 20, 4992, https://doi.org/10.3390/ijms20204992, 2019.

Crova, F., Forello, A. C., Bernardoni, V., Calzolai, G., Canepari, S., Argentini, S., Costabile, F., Frezzini, M. A., Giardi, F., Lucarelli, F., Massabò, D., Massimi, L., Nava, S., Paglione, M., Pazzi, G., Prati, P., Rinaldi, M., Russo, M., Valentini, S., Valli, G., Vernocchi, V., and Vecchi, R.: Assessing the role of atmospheric dispersion vs. emission strength in the southern Po Valley (Italy) using dispersion-normalised multi-time receptor modelling, Atmos. Environ., 316, 120168, https://doi.org/10.1016/j.atmosenv.2023.120168, 2024.

Dai, Q., Hopke, P. K., Bi, X., and Feng, Y.: Improving apportionment of $PM_{2.5}$ using multisite PMF by constraining G-values with apriori information, Sci. Total Environ., 736, 139657, https://doi.org/10.1016/j.scitotenv.2020.139657, 2020.

Dai, Q., Ding, J., Song, C., Liu, B., Bi, X., Wu, J., Zhang, Y., Feng, Y., and Hopke, P. K.: Changes in source contributions to particle number concentrations after the COVID-19 outbreak: Insights from a dispersion normalized PMF, Sci. Total Environ., 759, 143548, https://doi.org/10.1016/j.scitotenv.2020.143548, 2021.

Damayanti, S., Harrison, R. M., Pope, F., and Beddows, D. C. S.: Limited impact of diesel particle filters on road traffic emissions of ultrafine particles, Environ. Int., 174, 107888, https://doi.org/10.1016/j.envint.2023.107888, 2023.

de Jesus, A. L., Thompson, H., Knibbs, L. D., Kowalski, M., Cyrys, J., Niemi, J. V., Kousa, A., Timonen, H., Luoma, K., Petäjä, T., Beddows, D., Harrison, R. M., Hopke, P., and Morawska, L.: Long-term trends in $PM_{2.5}$ mass and particle number concentrations in urban air: the impacts of mitigation measures and extreme events due to changing climates, Environ. Pollut., 263, 114500, https://doi.org/10.1016/j.envpol.2020.114500, 2020.

EU EEA: Air pollution, https://www.eea.europa.eu/en/topics/in-depth/air-pollution (last access: 20 December 2023), 2023.

Harni, S. D., Aurtela, M., Saarikoski, S., Niemi, J., Portin, H., Manninen, H., Leinonen, V., Aalto, P., Hopke, P., Petäjä, T., Rönkkö, T., and Timonen, H.: Source apportionment of particle number size distribution at the street canyon and urban background sites, EGUsphere [preprint], https://doi.org/10.5194/egusphere-2023-2428, 2023.

Harrison, R. M., Beddows, D. C. S., and Dall'Osto, M.: PMF analysis of wide-range particle size spectra collected on a major highway, Environ. Sci. Technol., 45, 5522–5528, https://doi.org/10.1021/es2006622, 2011.

Harrison, R. M., MacKenzie, R. A., Xu, H., Alam, M. S., Nikolova, I., Zhong, J., Singh, A., Zeraati-Rezaei, S., Stark, C., Beddows, D. C. S., Liang, Z., Xu, R., and Cai, X.: Diesel exhaust nanoparticles and their behaviour in the atmosphere, Proc. R. Soc. A 474, https://doi.org/10.1098/rspa.2018.0492, 2018.

Harrison, R. M., Beddows, D. C. S., Alam, M. S., Singh, A., Brean, J., Xu, R., Kotthaus, S., and Grimmond, S.: Interpretation of particle number size distributions measured across an urban area during the FASTER campaign, Atmos. Chem. Phys., 19, 39–55, https://doi.org/10.5194/acp-19-39-2019, 2019.

HEI Review Panel on Ultrafine Particles: Understanding the health effects of ambient ultrafine particles, HEI Perspectives 3, Health Effects Institute, Boston, 2013.

Hersbach, H., Bell, B., Berrisford, P., Biavati, G., Horányi, A., Muñoz Sabater, J., Nicolas, J., Peubey, C., Radu, R., Rozum, I., Schepers, D., Simmons, A., Soci, C., Dee, D., and Thépaut, J-N.: ERA5 hourly data on single levels from 1940 to present. Copernicus Climate Change Service (C3S) Climate Data Store (CDS), https://doi.org/10.24381/cds.adbb2d47 (last access: 10 September 2023), 2023.

Holzworth, G. C.: Mixing depths, wind speeds and air pollution potential for selected locations in the United States, J. Appl. Meteor., 6, 1039–1044, https://doi.org/10.1175/1520-0450(1967)006<1039:mdwsaa>2.0.co;2, 1967.

Hopke, P. K.: An introduction to receptor modeling, Chemometr. Intell. Lab., 10, 21–43, https://doi.org/10.1016/0169-7439(91)80032-l, 1991.

https://doi.org/10.5194/egusphere-2024-316
Preprint. Discussion started: 13 February 2024

Hopke, P. K.: A guide to positive matrix factorization. https://people.clarkson.edu/~phopke/PMF-Guidance.htm (last access: 10 September 2023), 2000.

Hopke, P. K.: Review of receptor modeling methods for source apportionment, J. Air Waste Manage., 66, 237–259, https://doi.org/10.1080/10962247.2016.1140693, 2016.

Hopke, P. K., Dai, Q., Li, L., and Feng, Y.: Global review of recent source apportionments for airborne particulate matter, Sci. Total Environ., 740, 140091, https://doi.org/10.1016/j.scitotenv.2020.140091, 2020.

Hopke, P. K., Feng, Y., and Dai, Q.: Source apportionment of particle number concentrations: A global review, Sci. Total Environ., 819, 153104, https://doi.org/10.1016/j.scitotenv.2022.153104, 2022.

Hopke, P. K., Chen, Y., Rich, D. Q., Mooibroek, D., and Sofowote, U. M.: The application of positive matrix factorization with diagnostics to BIG DATA, Chemometr. Intell. Lab., 240, 104885, https://doi.org/10.1016/j.chemolab.2023.104885, 2023.

Ibald-Mulli, A., Wichmann, H.-E., Kreyling, W., and Peters, A.: Epidemiological evidence on health effects of ultrafine particles, J. Aerosol Med., 15, 189–201, https://doi.org/10.1089/089426802320282310, 2002.

Juozaitis, A., Trakumas, S., Girgždien, R., Girgždys, A., Šopauskien, D., and Ulevičius, V.: Investigations of gas-to-particle conversion in the atmosphere, Atmos. Res., 41, 183–201, https://doi.org/10.1016/0169-8095(96)00008-7, 1996.

Kadowaki, S.: Size distribution and chemical composition of atmospheric particulate nitrate in the Nagoya area, Atmos. Environ., 11, 671–675, https://doi.org/10.1016/0004-6981(77)90174-3, 1977.

Kerminen, V. M., Chen, X., Vakkari, V., Petäjä, T., Kulmala, M., and Bianchi, F.: Atmospheric new particle formation and growth: Review of field observations, Environ. Res. Lett., 13, 103003, https://doi.org/10.1088/1748-9326/aadf3c, 2018.

Ketzel, M. and Berkowicz, R.: Modelling the fate of ultrafine particles from exhaust pipe to rural background: an analysis of time scales for dilution, coagulation and deposition, Atmos. Environ., 38, 2639–2652, https://doi.org/10.1016/j.atmosenv.2004.02.020, 2004.

Kreyling, W. G., Semmler-Behnke, M., and Möller, W.: Ultrafine particle-lung interactions: does size matter? J. Aerosol Med., 19, 74–83, https://doi.org/10.1089/jam.2006.19.74., 2006.

Kumar, P., Ketzel, M., Vardoulakis, S., Pirjola, L., and Britter, R.: Dynamics and dispersion modelling of nanoparticles from road traffic in the urban atmospheric environment – A review, J. Aerosol Sci., 42, 580–603, https://doi.org/10.1016/j.jaerosci.2011.06.001, 2011.

Kulmala, M.: How particles nucleate and grow, Science, 302, 1000, https://doi.org/10.1126/science.1090848, 2003.

Kulmala, M., Petäjä, T., Ehn, M., Thornton, J., Sipilä, M., Worsnop, D. R., and Kerminen, V. M.: Chemistry of atmospheric nucleation: On the recent advances on precursor characterization and atmospheric cluster composition in connection with atmospheric new particle formation, Annu. Rev. Phys. Chem., 65, 21–37, https://doi.org/10.1146/annurev-physchem-040412-110014, 2014.

Kulmala, M., Lintunen, A., Lappalainen, H., Virtanen, A., Yan, C., Ezhova, E., Nieminen, T., Riipinen, I., Makkonen, R., Tamminen, J., Sundström, A.-M., Arola, A., Hansel, A., Lehtinen, K., Vesala, T., Petäjä, T., Bäck, J., Kokkonen, T., and Kerminen, V.-M.: Opinion: The strength of long-term comprehensive observations to meet multiple grand challenges in different environments and in the atmosphere, Atmos. Chem. Phys., 23, 14949–14971, https://doi.org/10.5194/acp-23-14949-2023, 2023.

Leahey, D. M.: An advective model for predicting air pollution within an urban heat island with applications to New York City, J. Air Waste Manag. Assoc., 22, 548–550, https://doi.org/10.1080/00022470.1972.10469678, 1972.

Li, Q.-Q., Guo, Y.-T., Yang, J.-Y., and Liang, C.-S.: Review on main sources and impacts of urban ultrafine particles: Traffic emissions, nucleation, and climate modulation, Atmos. Environ.: X, 19, 100221, https://doi.org/10.1016/j.aeaoa.2023.100221, 2023.

Liu, Z. R., Hu, B., Liu, Q., Sun, Y., and Wang, Y. S.: Source apportionment of urban fine particle number concentration during summertime in Beijing, Atmos. Environ., 96, 359–369, https://doi.org/10.1016/j.atmosenv.2014.06.055, 2014.

Maricq, M. M., Chase, R. E., Xu, N., and Laing, P. M.: The effects of the catalytic converter and fuel sulfur level on motor vehicle particulate matter emissions: Light duty diesel vehicles, Environ. Sci. Technol., 36, 283–289, https://doi.org/10.1021/es010962l, 2002.

Meng, X., Ma, Y., Chen, R., Zhou, Z., Chen, B., and Kan, H.: Size-fractionated particle number concentrations and daily mortality in a Chinese city, Environ. Health Perspect., 121, 1174–1178, https://doi.org/10.1289/ehp.1206398, 2013.

Mikkonen, S., Németh, Z., Varga, V., Weidinger, T., Leinonen, V., Yli-Juuti, T., and Salma, I.: Decennial time trends and diurnal patterns of particle number concentrations in a central European city between 2008 and 2018, Atmos. Chem. Phys., 20, 12247–12263, https://doi.org/10.5194/acp-20-12247-2020, 2020.

https://doi.org/10.5194/egusphere-2024-316
Preprint. Discussion started: 13 February 2024

Morawska, L., Ristovski, Z., Jayaratne, E. R., Keogh, D. U., and Ling, X.: Ambient nano and ultrafine particles from motor vehicle emissions: Characteristics, ambient processing and implications on human exposure, Atmos. Environ., 42, 8113–8138, https://doi.org/10.1016/j.atmosenv.2008.07.050, 2008.

Németh, Z. and Salma, I.: Spatial extension of nucleating air masses in the Carpathian Basin, Atmos. Chem. Phys., 14, 8841–8848, https://doi.org/10.5194/acp-14-8841-2014, 2014.

Oberdörster, G., Oberdörster, E., and Oberdörster, J.: Nanotoxicology: An emerging discipline evolving from studies of ultrafine particles, Environ. Health Perspect., 113, 823–839, https://doi.org/10.1289/ehp.7339, 2005.

Ogulei, D., Hopke, P. K., Chalupa, D., and Utell, M.: Modeling source contributions to submicron particle number concentrations measured in Rochester, NY, Aerosol Sci. Technol., 41, 179–201, https://doi.org/10.1080/02786820601116012, 2007.

Paatero, P.: The Multilinear Engine: A table-driven, least squares program for solving multilinear problems, including the n-way parallel factor analysis model, J. Comput. Graph. Statistics, 8, 854, https://doi.org/10.2307/1390831, 1999.

Paatero, P. and Tapper, U.: Analysis of different modes of factor analysis as least squares fit problems, Chemometr. Intell. Lab., 18, 183–194, https://doi.org/10.1016/0169-7439(93)80055-m, 1993.

Paatero, P. and Tapper, U.: Positive matrix factorization: A non-negative factor model with optimal utilization of error estimates of data values, Environmetrics, 5, 111–126, https://doi.org/10.1002/env.3170050203, 1994.

Pandolfi, M., Gonzalez-Castanedo, Y., Alastuey, A., de la Rosa, J. D., Mantilla, E., de la Campa, A. S., Querol, X., Pey, J., Amato, F., and Moreno, T.: Source apportionment of PM_{10} and $PM_{2.5}$ at multiple sites in the strait of Gibraltar by PMF: impact of shipping emissions, Environ. Sci. Pollut. Res., 18, 260–269, https://doi.org/10.1007/s11356-010-0373-4, 2010.

Riediker, M., Zink, D., Kreyling, W., Oberdörster, G., Elder, A., Graham, U., Lynch, I., Duschl, A., Ichihara, G., Ichihara, S., Kobayashi, T., Hisanaga, N., Umezawa, M., Cheng, T.-J., Handy, R., Gulumian, M., Tinkle, S., and Cassee, F.: Particle toxicology and health - where are we?, Part. Fibre Toxicol., 16, https://doi.org/10.1186/s12989-019-0302-8, 2019.

Rivas, I., Beddows, D. C. S., Amato, F., Green, D. C., Järvi, L., Hueglin, C., Reche, C., Timonen, H., Fuller, G. W., Niemi, J. V., Pérez, N., Aurela, M., Hopke, P. K., Alastuey, A., Kulmala, M., Harrison, R. M., Querol, X., and Kelly, F. J.: Source apportionment of particle number size distribution in urban background and traffic stations in four European cities, Environ. Int., 135, 105345, https://doi.org/10.1016/j.envint.2019.105345, 2020.

Robinson, A. L., Donahue, N. M., Shrivastava, M. K., Weitkamp, E. A, Sage, A. M., Grieshop, A. P., Lane, T. E., Pierce, J. R., and Pandis, S. N.: Rethinking organic aerosols: semivolatile emissions and photochemical aging, Science, 80, 315, 1259–1262, https://doi.org/10.1126/science.1133061, 2007.

Rowell, A., Brean, J., Beddows, D. C. S., Shi, Z., Petäjä, T., Vörösmarty, M., Salma, I., Niemi, J. V., Manninen, H. E., van Pinxteren, D., Harrison, R. M., Tuch, T., and Weinhold, K.: Insights into the sources of ultrafine particle numbers at six European urban sites obtained by investigating COVID-19 lockdowns, EGUsphere [preprint], https://doi.org/10.5194/egusphere-2023-3053, 2024.

Rönkkö, T., Kuuluvainen, H., Karjalainen, P., Keskinen, J., Hillamo, R., Niemi, J. V., Pirjola, L., Timonen, H. J., Saarikoski, S., Saukko, E., Järvinen, A., Silvennoinen, H., Rostedt, A., Olin, M., Yli-Ojanperä, J., Nousiainen, P., Kousa, A., Dal Maso, M.: Traffic is a major source of atmospheric nanocluster aerosol, Proc. Natl. Acad. Sci., 114, 7549–7554. https://doi.org/10.1073/pnas.1700830114, 2017.

Rönkkö, T. and Timonen, H.: Overview of sources and characteristics of nanoparticles in urban traffic-influenced areas, J. Alzheimer's Dis., 72, 15–28, https://doi.org/10.3233/jad-190170, 2019.

Salma, I. and Németh, Z.: Dynamic and timing properties of new aerosol particle formation and consecutive growth events, Atmos. Chem. Phys., 19, 5835–5852, https://doi.org/10.5194/acp-19-5835-2019, 2019.

Salma, I., Maenhaut, W., and Záray, Gy.: Comparative study of elemental mass size distributions in urban atmospheric aerosol, J. Aerosol Sci., 33, 339–356, https://doi.org/10.1016/S0021-8502(01)00176-8, 2002.

Salma, I., Maenhaut, W., Chi, X., Ocskay, R., Záray, Gy.: Mass size distribution of particulate matter in the urban atmosphere, J. Aerosol Sci., 34S1, 693–694, 2003.

Salma, I., Borsós, T., Weidinger, T., Aalto, P., Hussein, T., Dal Maso, M., and Kulmala, M.: Production, growth and properties of ultrafine atmospheric aerosol particles in an urban environment, Atmos. Chem. Phys., 11, 1339–1353, https://doi.org/10.5194/acp-11-1339-2011, 2011.

Salma, I., Füri, P., Németh, Z., Farkas, Á., Balásházy, I., Hofmann, W., and Farkas, Á.: Lung burden and deposition distribution of inhaled atmospheric urban ultrafine particles as the first step in their health risk assessment, Atmos. Environ., 104, 39–49, https://doi.org/10.1016/j.atmosenv.2014.12.060, 2015.

https://doi.org/10.5194/egusphere-2024-316
Preprint. Discussion started: 13 February 2024

Salma, I., Németh, Z., Weidinger, T., Kovács, B., and Kristóf, G.: Measurement, growth types and shrinkage of newly formed aerosol particles at an urban research platform, Atmos. Chem. Phys., 16, 7837–7851, https://doi.org/10.5194/acp-16-7837-2016, 2016a.

Salma, I., Németh, Z., Kerminen, V.-M., Aalto, P., Nieminen, T., Weidinger, T., Molnár, Á., Imre, K., and Kulmala, M.: Regional effect on urban atmospheric nucleation, Atmos. Chem. Phys., 16, 8715–8728, https://doi.org/10.5194/acp-16-8715-2016, 2016b.

Salma, I., Vörösmarty, M., Gyöngyösi, A. Z., Thén, W., and Weidinger, T.: What can we learn about urban air quality with regard to the first outbreak of the COVID-19 pandemic? A case study from central Europe, Atmos. Chem. Phys., 20, 15725–15742, https://doi.org/10.5194/acp-20-15725-2020, 2020.

Salma, I., Thén, W., Aalto, P., Kerminen, V.-M., Kern, A., Barcza, Z., Petäjä, T., and Kulmala, M.: Influence of vegetation on occurrence and time distributions of regional new aerosol particle formation and growth, Atmos. Chem. Phys., 21, 2861–2880, https://doi.org/10.5194/acp-21-2861-2021, 2021.

Shi, J. P. and Harrison, R. M.: Investigation of ultrafine particle formation during diesel exhaust dilution, Environ. Sci. Technol. 33, 3730–3736. https://doi.org/10.1021/ es981187l, 1999.

Squizzato, S., Masiol, M., Emami, F., Chalupa, D., Utell, M., Rich, D., and Hopke, P.: Long-term changes of source apportioned particle number concentrations in a metropolitan area of the northeastern United States, Atmosphere, 10, 27, https://doi.org/10.3390/atmos10010027, 2019.

Souza, C. R.: The Accord.NET Framework, http://accord-framework.net (last access: 10 September 2023), 2014.

Teinilä, K., Timonen, H., Aurela, M., Kuula, J., Rönkkö, T., Hellèn, H., Loukkola, K., Kousa, A., Niemi, J. V., and Saarikoski, S.: Characterization of particle sources and comparison of different particle metrics in an urban detached housing area, Finland, Atmos. Env., 272, 118939, https://doi.org/10.1016/j.atmosenv.2022.118939, 2022.

Thén, W. and Salma, I.: Particle number concentration: a case study for air quality monitoring, Atmosphere, 13, 570, https://doi.org/10.3390/atmos13040570, 2022.

Trechera, P., Garcia-Marlès, M., Liu, X., Reche, C., Pérez, N., Savadkoohi, M., Beddows, D., Salma, I., Vörösmarty, M., Casans, A., Casquero-Vera, J. A., Hueglin, C., Marchand, N., Chazeau, B., Gille, G., Kalkavouras, P., Mihalopoulos, N., Ondracek, J., Zikova, N., Niemi, J. V., Manninen, H. E., Green, D. C., Tremper, A. H., Norman, M., Vratolis, S., Eleftheriadis, K., Gómez-Moreno, F. J., Alonso-Blanco, E., Gerwig, H., Wiedensohler, A., Weinhold, K., Merkel, M., Bastian, S., Petit, J.-E., Favez, O., Crumeyrolle, S., Ferlay, N., Martins Dos Santos, S., Putaud, J.-P., Timonen, H., Lampilahti, J., Asbach, C., Wolf, C., Kaminski, H., Altug, H., Hoffmann, B., Rich, D. Q., Pandolfi, M., Harrison, R. M., Hopke, P. K., Petäjä, T., Alastuey, A., and Querol, X.: Phenomenology of ultrafine particle concentrations and size distribution across urban Europe, Environ. Int., 172, 107744, https://doi.org/10.1016/j.envint.2023.107744, 2023.

Uria-Tellaetxe, I. and Carslaw, D. C.: Conditional bivariate probability function for source identification, Environ. Modell. Softw., 59, 1–9, https://doi.org/10.1016/j.envsoft.2014.05.002, 2014.

US EPA: Positive matrix factorization model for environmental data analyses, https://www.epa.gov/air-research/positive matrix-factorization-model-environmental-data-analyses (last access: 10 September 2023), 2014.

US EPA: Criteria air pollutants, https://www.epa.gov/criteria-air-pollutants (last access: 20 December 2023), 2023.

Vu, T. V., Delgado-Saborit, J. M., and Harrison, R. M.: Review: Particle number size distributions from seven major sources and implications for source apportionment studies, Atmos. Env., 122, 114–132, https://doi.org/10.1016/j.atmosenv.2015.09.027, 2015.

Vratolis, S., Gini, M. I., Bezantakos, S., Stavroulas, I., Kalivitis, N., Kostenidou, E., Louvaris, E., Siakavaras, D., Biskos, G., Mihalopoulos, N., Pandis, S. N., Pilinis, C., Papayannis, A., and Eleftheriadis, K.: Particle number size distribution statistics at city-centre urban background, urban background, and remote stations in Greece during summer, Atmos. Environ., 213, 711–726, https://doi.org/10.1016/j.atmosenv.2019.05.064, 2019.

Viana, M., Kuhlbusch, T. A. J., Querol, X., Alastuey, A., Harrison, R. M., Hopke, P. K., Winiwarter, W., Vallius, M., Szidat, S., Prévôt, A. S. H., Hueglin, C., Bloemen, H., Wåhlin, P., Vecchi, R., Miranda, A. I., Kasper-Giebl, A., Maenhaut, W., and Hitzenberger, R.: Source apportionment of particulate matter in Europe: A review of methods and results, J. Aerosol Sci. 39, 827–849, https://doi.org/10.1016/j.jaerosci.2008.05.007, 2008.

Wiedensohler, A., Birmili, W., Nowak, A., Sonntag, A., Weinhold, K., Merkel, M., Wehner, B., Tuch, T., Pfeifer, S., Fiebig, M., Fjäraa, A. M., Asmi, E., Sellegri, K., Depuy, R., Venzac, H., Villani, P., Laj, P., Aalto, P., Ogren, J. A., Swietlicki, E., Williams, P., Roldin, P., Quincey, P., Hüglin, C., Fierz-Schmidhauser, R., Gysel, M., Weingartner, E., Riccobono, F., Santos, S., Grüning, C., Faloon, K., Beddows, D., Harrison, R., Monahan, C., Jennings, S. G., O'Dowd, C. D., Marinoni, A., Horn, H.-G., Keck, L., Jiang, J., Scheckman, J., McMurry, P. H., Deng, Z., Zhao, C. S., Moerman, M., Henzing, B.,

https://doi.org/10.5194/egusphere-2024-316
Preprint. Discussion started: 13 February 2024

de Leeuw, G., Löschau, G., and Bastian, S.: Mobility particle size spectrometers: harmonization of technical standards and data structure to facilitate high quality long-term observations of atmospheric particle number size distributions, Atmos. Meas. Tech., 5, 657–685, https://doi.org/10.5194/amt-5-657-2012, 2012.

Wang, M., Hopke, P. K., Masiol, M., Thurston, S. W., Cameron, S., Ling, F., van Wijngaarden, E., Croft, D., Squizzato, S., Thevenet-Morrison, K., Chalupa, D., and Rich, D. Q.: Changes in triggering of ST-elevation myocardial infarction by particulate air pollution in Monroe County, New York over time: a case-crossover study, Environ. Health., 18, 82, https://doi.org/10.1186/s12940-019-0521-3, 2019a.

Wang, K., Nakao, S., Thimmaiah, D., and Hopke, P. K.: Emissions from in-use residential wood pellet boilers and potential emissions savings using thermal storage, Sci. Total Environ., 676, 564–576, https://doi.org/10.1016/j.scitotenv.2019.04.325, 2019b.

WHO Global Air Quality Guidelines: Particulate matter ($PM_{2.5}$ and PM_{10}), ozone, nitrogen dioxide, sulfur dioxide and carbon monoxide, https://www.ncbi.nlm.nih.gov/books/NBK574594/, World Health Organization (last access: 10 September 2023), 2021.

Yoshizumi, K.: Regional size distributions of sulfate and nitrate in the Tokyo metropolitan area in summer, Atmos. Environ., 20, 763–766, https://doi.org/10.1016/0004-6981(86)90191-5, 1986.

Zhang, Y., Zhang, Q., Yao, Z., and Li, H.: Particle size and mixing state of freshly emitted black carbon from different combustion sources in China, Environ. Sci. Technol., 54, 7766–7774, https://doi.org/10.1021/acs.est.9b07373, 2020.

Zhou, L., Kim, E., Hopke, P. K., Stanier, C., and Pandis, S. N.: Advanced factor analysis on Pittsburgh particle size-distribution data, Aerosol Sci. Technol., 38, 118–132, https://doi.org/10.1080/02786820390229589, 2004.